ELSEVIER

Contents lists available at ScienceDirect

# **Transportation Engineering**

journal homepage: www.sciencedirect.com/journal/transportation-engineering



## Validation, interpretation and use of railway track acceleration data

William Powrie a, David Milne, Geoff Watson, Ben Lee, Louis Le Pen, Court Lee, David Milne, Geoff Watson, Ben Lee

- a University of Southampton, Department of Civil, Maritime and Environmental Engineering, Boldrewood Innovation Campus, Burgess Road, Southampton SO16 7QF, UK
- <sup>b</sup> Network Rail Infrastructure Limited, Network Rail, Waterloo General Office, London, SE1 8SW, UK
- c Ramboll, Twenty3 Brunswick Place, Southampton SO15 2AQ, UK

#### ARTICLE INFO

Keywords: Railway track Accelerometers Train loading Track deflection Measurement

#### ABSTRACT

It has for many years been relatively straightforward to attach an accelerometer to a railway track and obtain data of track accelerations as trains pass. However, not all devices are suitable and there are a number of potential pitfalls in processing and interpreting the signal. The Paper discusses these, starting with issues associated with the measurement itself including the frequency of sampling, filtering and noise. Aspects of interpretation and use of train signature data are then considered. Areas of current debate and disagreement are highlighted, and some degree of resolution proposed, with reference to original and published data. This resolution, and new data on the performance of a complex set of switches and crossings, are the significant contributions to current knowledge.

## Railway track deflection measurement, then and now

Early days

Interest in the use of accelerometers to quantify vertical track movement during train passage can be traced at least as far back as the paper by Bowness *et al.* [2]. Attempts to use accelerometers in the field led to the conclusion that at that time they were too inaccurate for quantifying track movements. The signals were generally too noisy and the need to integrate the signal twice (from acceleration to displacement) introduced considerable uncertainty. Hence Bowness et al. [2] focused on two alternative techniques, as follows.

The first and more direct was the analysis of digital images captured using a 30 frame/second video camera – the fastest affordable at the time. The camera would be located at a sufficient distance from the track to avoid higher frequency ground vibrations and also train aerodynamic effects, and sighted through an astronomical telescope onto targets placed either on the sleeper or on the rail. This technique was suitable for train speeds up to about 100 km/hour. Above this train speed, the camera framerate captured too few images within a cycle, leading to the potential for aliasing.

For train speeds greater than about 100 km/hour, low frequency geophones giving a linear velocity-voltage response above their natural frequency of about 2.5 Hz mounted onto the sleepers were used. Fig. 1a

and b show a typical geophone response. In addition to the initial non-linear sensitivity up to about 2.5 Hz, there is also a phase lag in the signal. The data (Fig. 1c) therefore had to be deconvoluted (Fig. 1d) to correct for these effects, and the signal low pass filtered to eliminate the high frequency vibrations (> about 40 Hz) not relevant to the assessment of track movement and high pass filtered for stability of the integration. To confirm that the signal processing was appropriate, and did not introduce artifacts or eliminate important effects, the approach was validated with reference to data from linear variable displacement transducers (LVDTs) on a laboratory actuator, and direct video image capture and analysis of field data. Processing to account for underlying response nonlinearity now tends to happen electronically within the transducer, but filtering the geophone signal to remove frequencies above about 40 Hz still occurs because it is frequencies below 40 Hz, even at the highest train speeds, that govern track deflection.

Over the past 20 years, transducer technology has improved and MEMS accelerometers now offer a viable, research-quality approach. They are robust, compact, inexpensive and can be self-logging. They are also much less noisy than previously, and are especially suitable for monitoring track movement under higher-speed trains. Fig. 2a–d shows the results of validation exercises, comparing the displacement against time traces for  $\pm 3$  g and  $\pm 16$  g accelerometers at different excitation frequencies, with geophones. Fig. 2e shows the displacement against time traces during the passage of a six-vehicle train travelling at 60 m/s,

E-mail address: wp@soton.ac.uk (W. Powrie).

<sup>\*</sup> Corresponding author at: University of Southampton, Department of Civil, Maritime and Environmental Engineering, Boldrewood Innovation Campus, Burgess Road, Southampton SO16 7QF, UK.

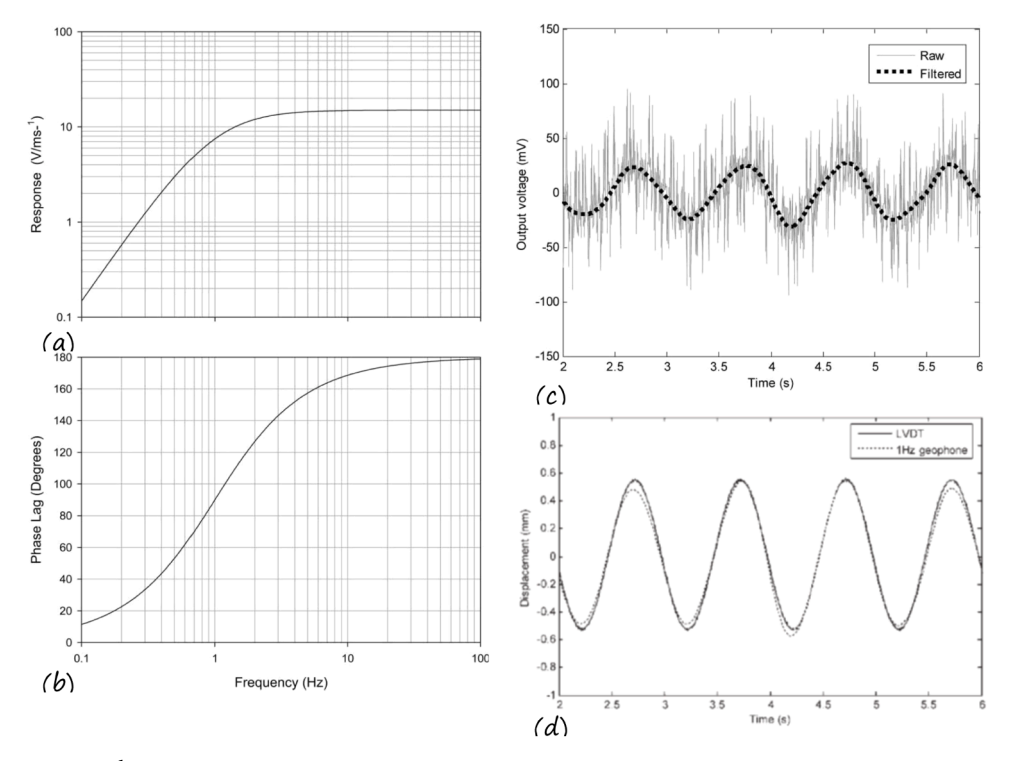


Fig. 1. (a) Typical response  $(V/ms^{-1})$  and (b) phase lag of an LF-24 low frequency geophone; (c) raw and filtered output voltage data and (d) integrated, filtered geophone results with full deconvolution from a LF-24 geophone during laboratory validation (amplitude  $\pm 0.5$  mm, frequency 1 Hz). From Bowness et al. [2].

determined using a geophone and a  $\pm$  16 g accelerometer. In the frequency domain (Fig. 2f), there is a small discrepancy between the traces at around 10 - 15 Hz owing to noise in the accelerometer. However, this is already at too high a frequency to affect the displacements significantly.

Fig. 3 shows some typical devices.

## Field deployment

A typical recent field deployment of 100 triaxial accelerometers to investigate the behaviour of one of a set of complex switches and crossings is illustrated in Fig. 4a. The accelerometers were fixed to bearers at various locations along the length of the switch and crossing, as indicated. The raw data were processed to give vertical and lateral accelerations (shown in Fig. 4b and c) during train passage. Data for two different types of train are illustrated; a bi-mode Intercity Express Train (IET) and a diesel-powered high speed train (HST). The IET at this location was operating on diesel power. Apart from differences in train geometry (in particular, vehicle length), the traction power units (diesel engines) are distributed along the length of the IET, while the HST has a large diesel engine in a dedicated power car at each end. The data have been filtered to two different maximum frequencies, 40 Hz and 200 Hz. This illustrates the frequency dependence for peak values of acceleration.

Fig. 4 shows that the biggest accelerations occur at features such as welds, the crossing nose and insulated joints. Thus nearly all of these peaks in acceleration are associated with something that disturbs the train on its passage through the crossing. There is some difference between the two train types, but filtering to 200 Hz gives much larger acceleration magnitudes than filtering to 40 Hz. However, accelerations at frequencies above 40 Hz do not have much effect on the displacement. For calculating track movements under load, filtering acceleration at frequencies greater than 40 Hz is appropriate. Higher frequency accelerations may be relevant for other purposes, in particular the effect on the train or ride quality.

## Analysis of track deflections: beam on an elastic foundation

Analysis of track performance is usually with reference to the classic beam on an elastic foundation [12], which treats the rail as a beam of flexural rigidity EI and models the entire support system – the ground, ballast, under sleeper pads and rail pads – as a bed of springs in series with an effective support system modulus k, defined as the load per unit length along the rail that causes a unit deflection.

Some care is needed with this definition, because we usually measure deflections at the sleeper rather than at the rail. Thus the effect of the rail pads is not included in the measurements, and needs to be added in manually when determining the rail support system stiffness as seen by a train. The approach models the sleeper support, which is in reality intermittent, as continuous along the track, but numerous studies have shown this to be a reasonable approximation for conventional 200 mm wide sleepers placed at 600 mm centres.

The other main potential limitations of the beam on an elastic foundation analysis as conventionally carried out are that it does not include the track or subgrade mass, hence will not model ground or track inertia, or damping. It also assumes that the rail support system modulus is reasonably uniform along the track, and does not cope well with hanging sleepers or a sudden localized change in rail support system stiffness [11]. In most circumstances these are not significant issues. In any case, the beam on an elastic foundation approach can be adapted and numerical approaches used to include any of them if needed, for example if a more faithful reproduction of measured track movements were required. A useful review of methods is presented by Lamprea-Pineda et al. [3].

## Interpretation and use of accelerometer data

Automatic compensation for processing drift

Accelerometer data may be plotted in the time domain (acceleration as a function of time, Fig. 5a), and in the frequency domain (acceleration

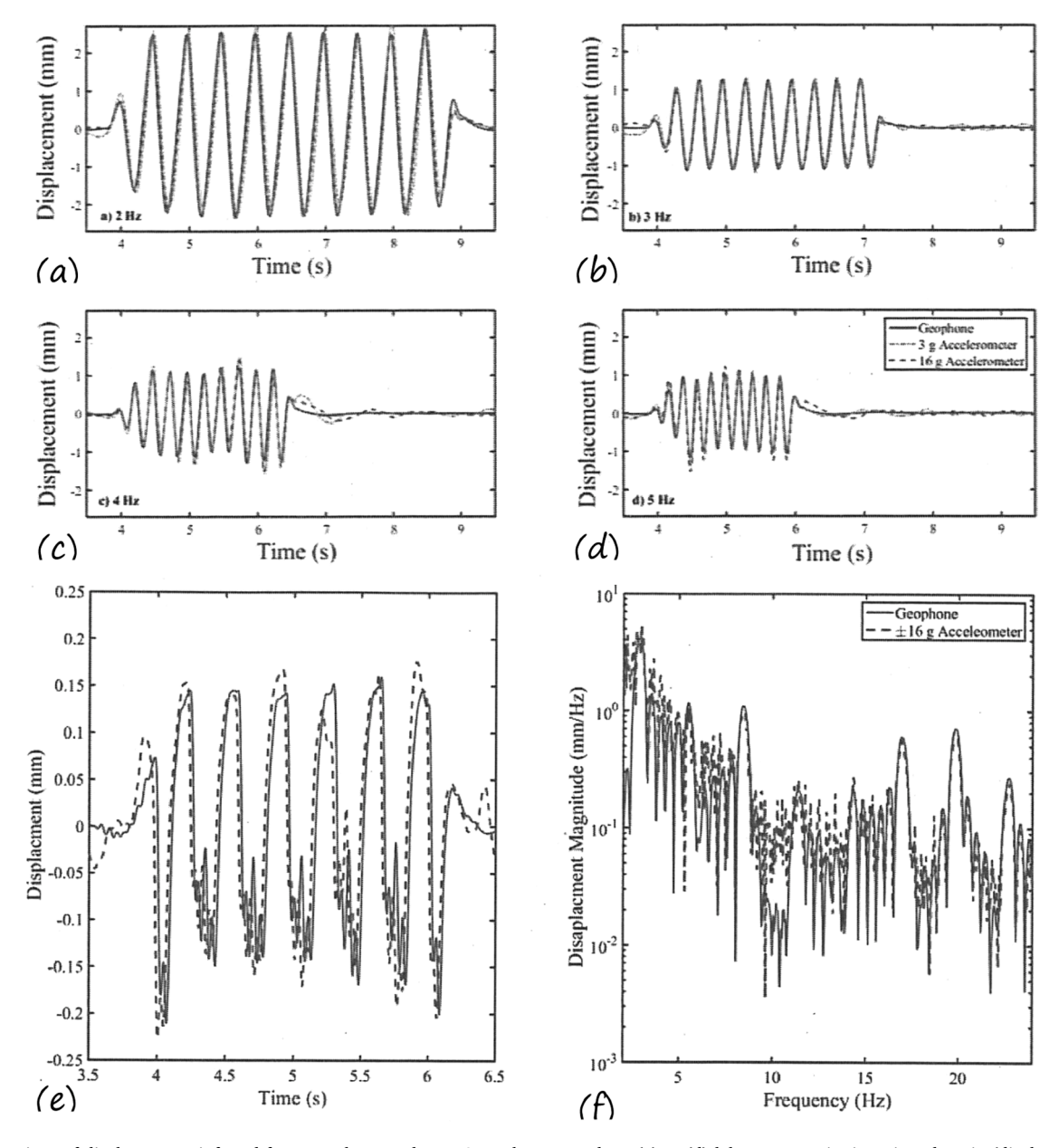


Fig. 2. Comparison of displacements inferred from geophone and MEMS accelerometer data. (a) to (d) laboratory excitation, time domain (displacement against time) at 2, 3, 4 and 5 Hz; (e) field deployment, time domain; (f) field deployment, frequency domain.

From Milne et al. [6].

as a function of frequency, Fig. 5b). Integrating the accelerations twice gives the displacement-time history (Fig. 5c). In the time domain plots (Fig. 5a and 5c) the loading effect of each individual axle is clear. However between Fig. 5a and 5c there is an upward drift in the datum position on performing each signal integration. This is an artefact of the high-pass filter being applied to a transient signal, and needs to be accounted for in analysing results obtained in this way.

Comparison with directly determined displacements on track or in the laboratory shows that the characteristic deflection during passage of a train is approximately the peak-to-peak distance, between the two dotted lines shown in what might be termed the stationary region on Fig. 5c. The apparent shift in the datum at the start of the trace is also indicated, along with the return to the true zero position at the end of the trace.

It is possible to extract each characteristic deflection manually, but this becomes time consuming when there are many train measurements to process. It also introduces a degree of subjectivity. Alternatively, estimation of the true track zero position can be automated through consideration of the cumulative distribution of displacement. Fig. 6a shows the normalized deflection of the track during a wheel passage, according to the beam on an elastic foundation analysis. Normalization is relative to the peak deflection, which is set to -1. Fig. 6a can be plotted as a distribution function or a probability density function, that is as the proportion of the cycle over which the deflection is greater (more negative) than the value in question. Thus there is zero probability that the normalized displacement will be more negative than -1, and certainty (p=1) that the displacement will be more negative than the small maximum uplift calculated just ahead of the wheel or axle. The true datum level is associated with and identifiable by a quite sharp knuckle in the data, at p=0.7. This gives a way of automatically identifying the true datum for determining track deflections.

Data from a real site are compared with results of a corresponding beam on an elastic foundation model for a particular type of train (a Javelin) in Fig. 7. In the time domain, the upward drift in the datum

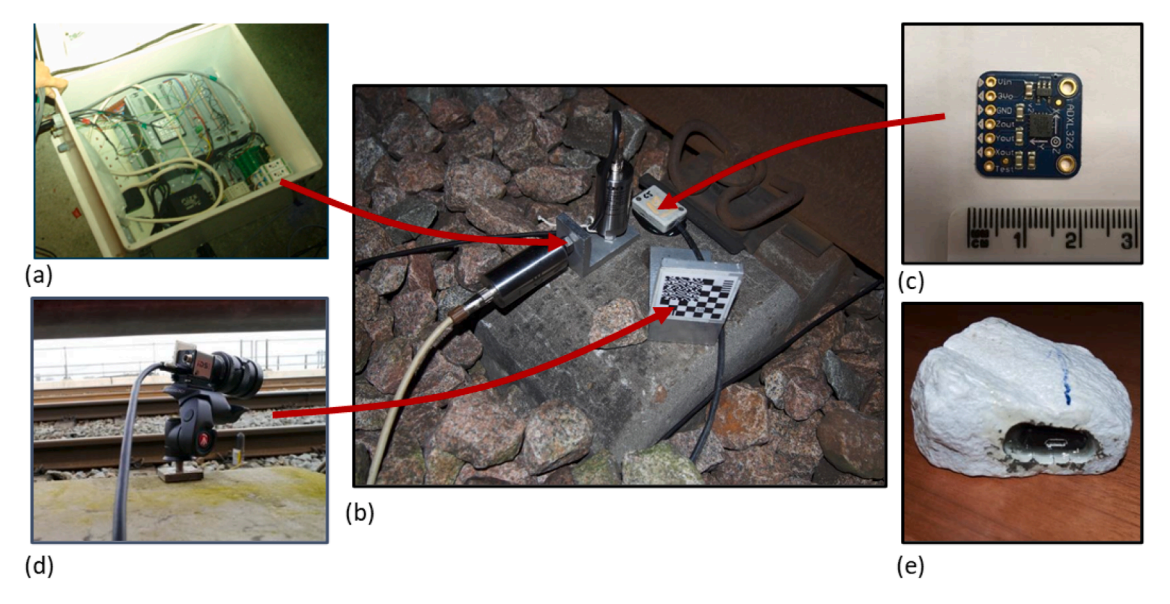


Fig. 3. Typical track deflection measurement devices: (a) geophone datalogger; (b) geophones, oriented to measure lateral and vertical velocity; (c) a MEMS accelerometer <2 cm in its largest dimension, which can be mounted in a housing (b), or inside a ballast stone (e) to measure accelerations in the ballast; (d) a video camera clamped onto a remote location sighting onto a target that is fixed rigidly to the sleeper.

position in the real accelerometer data (Fig. 7a) are absent from the model data (Fig. 7b). Comparing the density functions (Fig. 7c), the real data are displaced to the right (because of the datum drift) and the knuckle is not as sharp as in the model. Nonetheless, the true datum position can be identified reasonably accurately at a corresponding probability p of about 0.7.

The spectrum in the frequency domain is discussed later, with reference to train speed and key (vehicle, bogie and axle) passing frequencies.

### Field deployment and application

Monitoring using MEMS accelerometers with automated identification of the datum position was used in connection with the remediation of a particular defect that was proving resistant to repair by conventional machine tamping. At the location in question, the sleepers transition from monoblock to duo block and there are also some under-track crossings for cable ducts present. The whiteness in the ballast shown in Fig. 8 is an indication of excessive track movement, causing some disturbance and damage to the ballast grains. Normally this would be addressed by tamping, but in this case running the tamper through the site had no beneficial effects, and in some instances exacerbated the problem.

A number of accelerometers were installed, as shown in Fig. 8b and c. These were monitored over a period of time to assess the deflection of each sleeper during train passage. The data were used to determine how much each sleeper would be raised during manual re-packing of the ballast underneath. The accelerometers then remained in place to assess the efficacy of the repair.

Data of individual sleeper displacements during the monitoring campaign are shown in Fig. 9. Each individual cross in Fig. 9a–c represents the characteristic displacement of the sleeper during an individual train passage. Fig. 9a–c show various patterns of deterioration before and after both tamping and targeted remediations. What is clear is that routine tamping resulted at best in only a temporary improvement, and in one case (the mid-defect 6 ft sleeper) exacerbated the problem. Conversely, the targeted intervention successfully remediated the defect, effecting a lasting repair in every case. The adverse effect of routine tamping is further illustrated by the displacement-time histories shown in Figs. 9d and e.

This case study demonstrates the utility of the accelerometers and

processing methods in terms of understanding sleeper behavior, designing appropriate remediation solutions and demonstrating the effectiveness of the repair. Their low cost and ease of installation makes MEMS accelerometers equally suitable for monitoring and gaining insights into the factors affecting the behavior of long lengths of track, in the order of hundreds of sleepers [5,10].

### Characterization of train loading

It can be shown (see, for example, [7]) that for a train modelled as a series of moving axle loads, the classical beam on an elastic foundation solution has two components. These are (i) a shape function, giving the response to a single unit load in terms of deflection w with time t (or distance x)

$$w(t) = \frac{1}{2kL} e^{-\frac{\nu|t|}{L}} \left( \cos\left(\frac{\nu|t|}{L}\right) + \sin\left(\frac{\nu|t|}{L}\right) \right)$$
 (1)

and (ii) a loading function p(x,t), corresponding to the train of N appropriately-spaced loads  $(F_n,$  at spacings  $d_n)$  passing at the given velocity (v)

$$p(x,t) = \sum_{n=1}^{N} F_n(\delta(x - d_n - \nu t))$$
 (2)

Combining these gives the expression for the deflection of the track during train passage, as a function of time or distance:

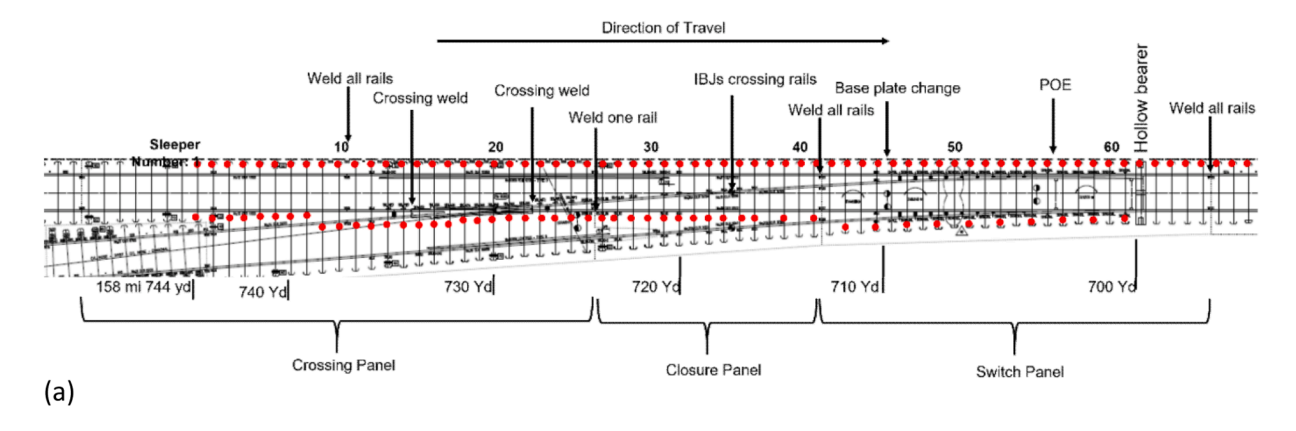
$$w(t) = \sum_{n=1}^{N} \frac{F_n}{2kL} e^{-\frac{|vt - d_n|}{L}} \left( \cos\left(\frac{|vt - d_n|}{L}\right) + \sin\left(\frac{|vt - d_n|}{L}\right) \right)$$
(3)

k (in MN/m<sup>2</sup>) is the load per unit length along the track that causes a unit deflection (the track support system modulus) and

$$L = \sqrt[4]{\frac{4EI}{k}} \tag{4}$$

is known as the characteristic length. *EI* (MN.m<sup>2</sup>) is the flexural rigidity (bending stiffness) of a single rail.

Modern trains are generally made up of a number of similar vehicles, hence start to take on a periodic form. An infinitely long periodic train has a load function



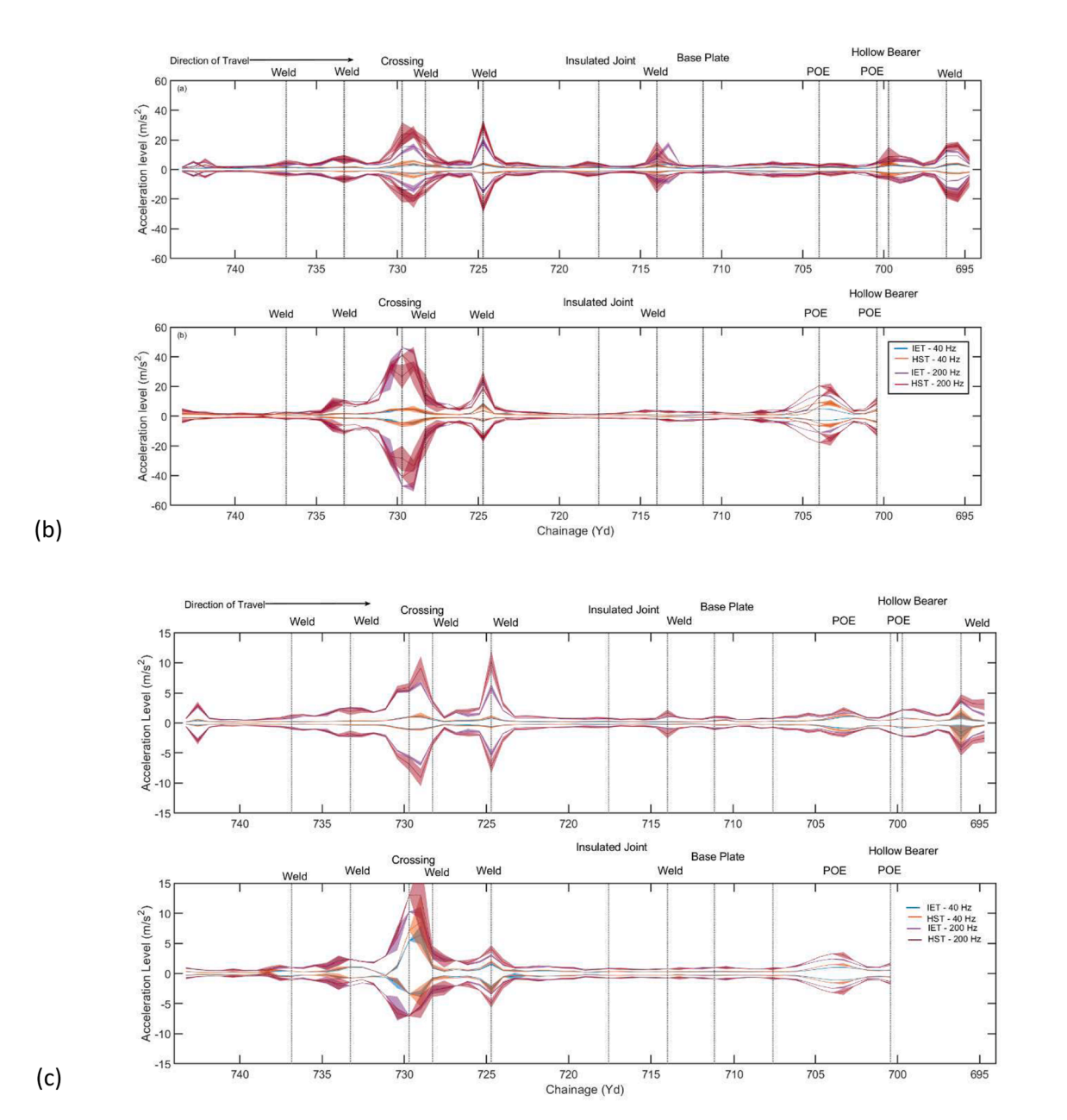


Fig. 4. (a) Layout of triaxial accelerometers at Cogload Junction, near Taunton; and typical measured (b) vertical and (c) lateral accelerations, filtered to 40 Hz and 200 Hz.

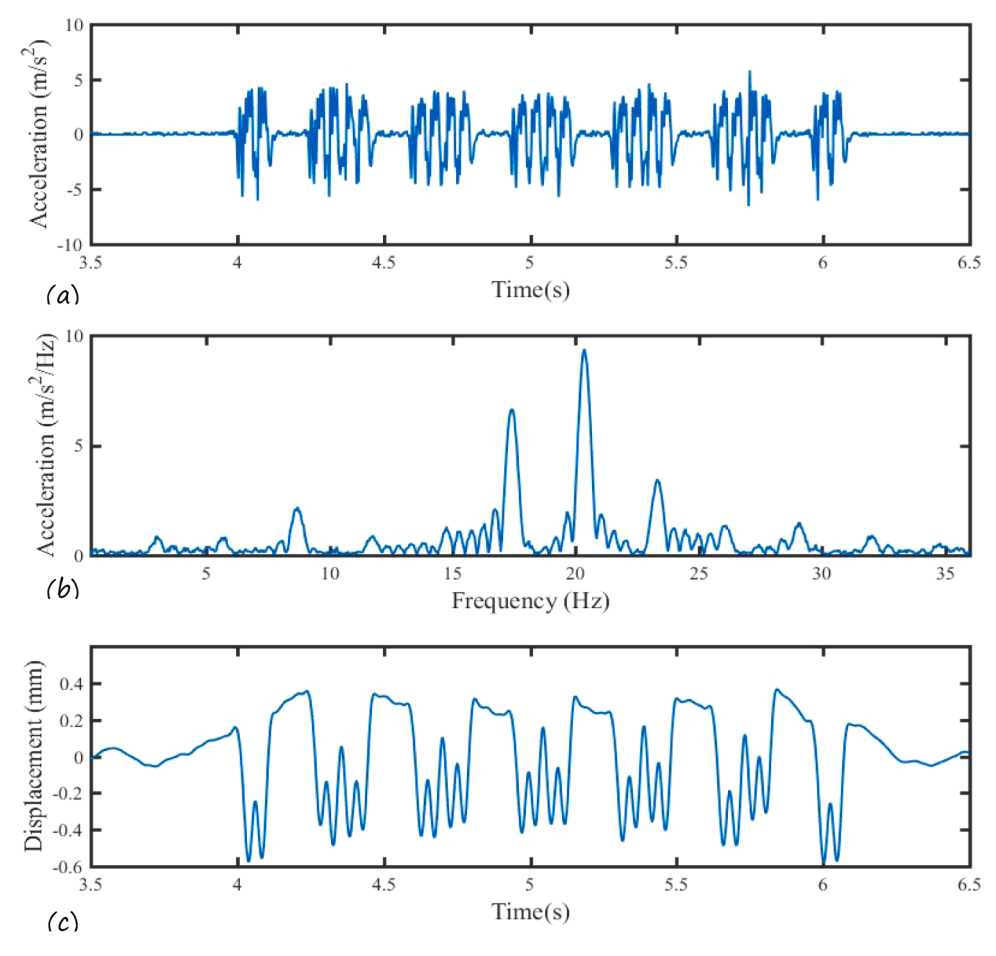


Fig. 5. Acceleration data in the (a) time and (b) frequency domains, and (c) displacements in the time domain, showing the apparent shift in datum as a result of signal processing (filtering and integration).

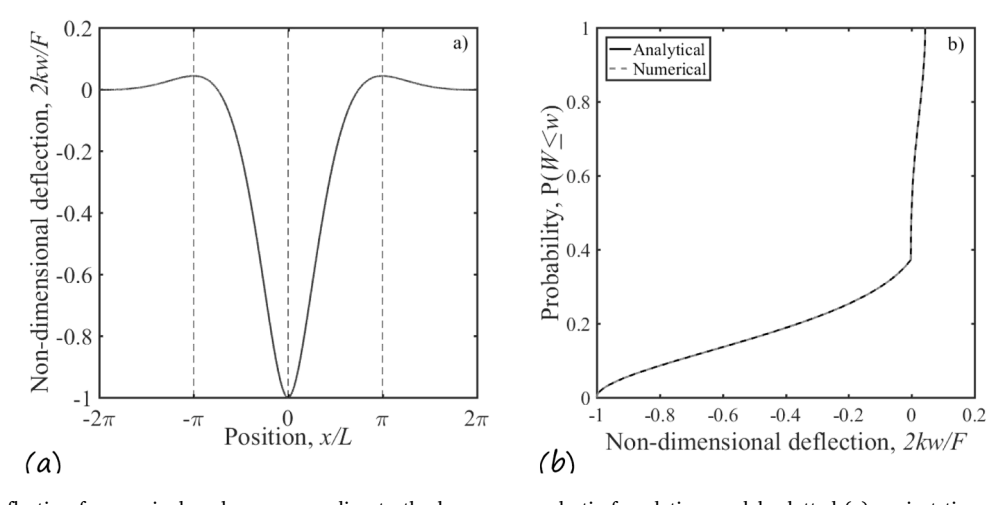


Fig. 6. Normalized deflection from a single axle pass according to the beam on an elastic foundation model, plotted (a) against time and (b) as a cumulative probability density function.

From Milne et al. [8].

$$f(t) = \sum_{n = -\infty}^{\infty} U_N e^{-\frac{i2\pi N vt}{L_v}}$$
 (5)

with

$$U_{N} = 4F \frac{v}{L_{\nu}} \left( \cos \left( \frac{\pi N L_{b}}{L_{\nu}} \right) \cdot \cos \left( \frac{\pi N L_{w}}{L_{\nu}} \right) \right)$$
 (6)

where F is the wheel load,  $L_v$  is the vehicle length,  $L_b$  is the bogic spacing (between centres) and  $L_w$  is the axle spacing within each bogic.

The load spectrum for a single vehicle is made up of contributions representing the bogie and the axle spacings, as illustrated in Fig. 10. Convolution of the axle and bogie-related spectra results in the effective scaling of the bogie spectrum by the generally higher-frequency axle spectrum, and "cancellation points" (at just under 4 and about 11.6

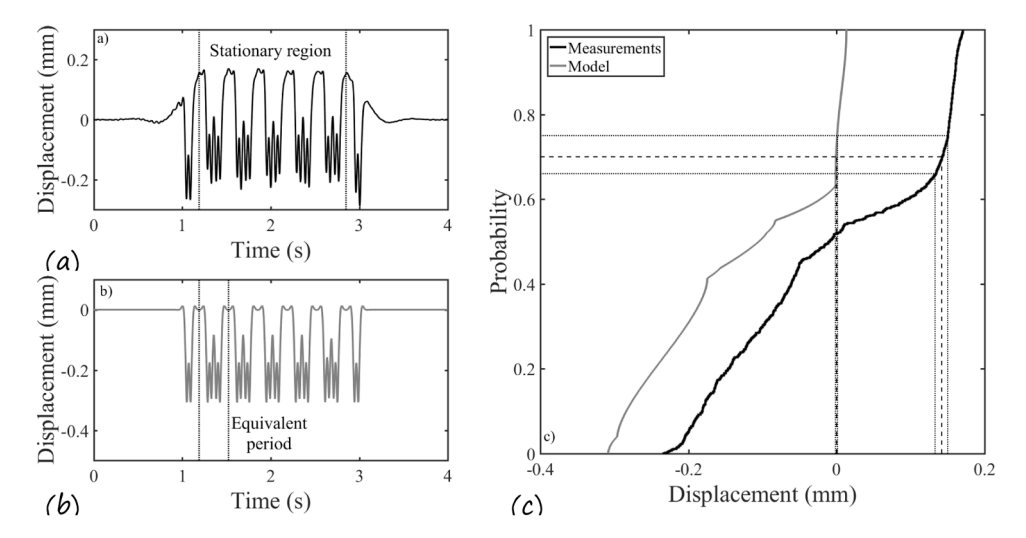


Fig. 7. (a) Measured and (b) calculated time domain displacements for a Javelin train, and (c) corresponding cumulative probability density functions. From Milne et al. [8].

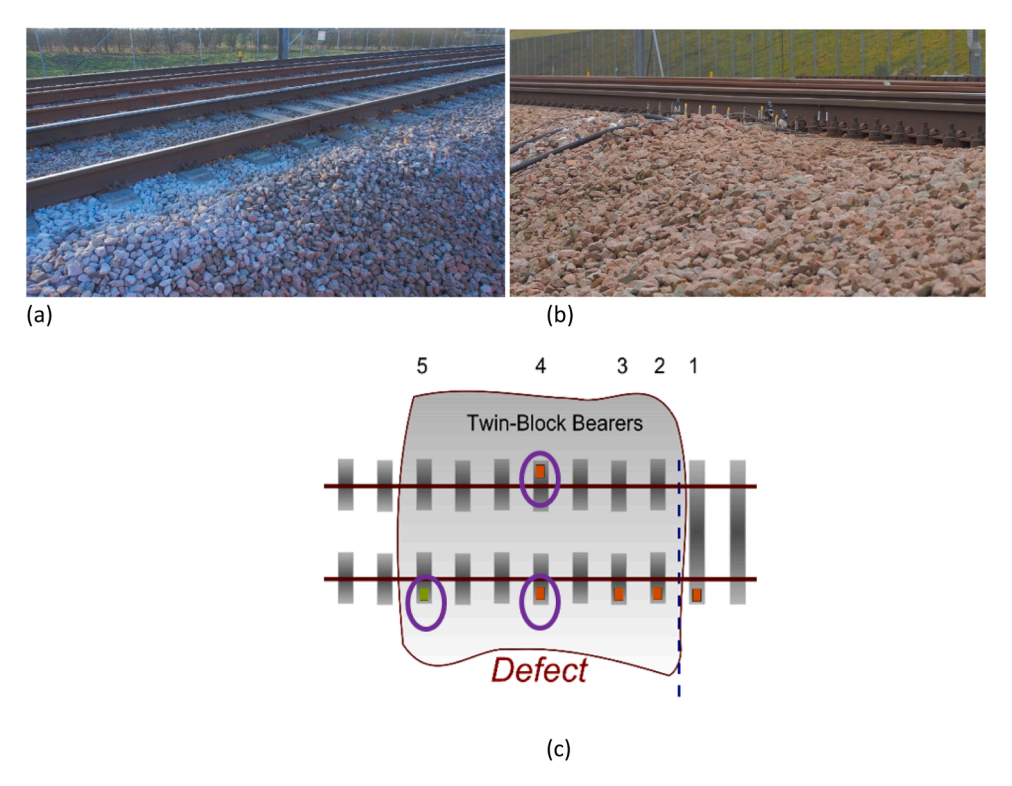


Fig. 8. Track defect site; (a) general view showing white spotting of ballast, (b) general view and (c) schematic plan of instrumentation. From Milne et al. [9].

times the vehicle passing frequency in this case) at which the resultant spectrum is zero (Fig. 10c).

As the number of vehicles in the train is increased, principal peak frequencies emerge at integer multiples of the vehicle passing frequency (Fig. 11).

This was first noted by Auersch [1], and is clear in measured vibration spectra including those presented by Milne *et al.* [7] (Fig. 12: these are for velocity rather than acceleration, but the same principles apply) and by Tang *et al.* [14].

Le Pen *et al.* [4] show that, for a given type of train, the rail support system stiffness can be determined from the ratio of the 3rd to the 7th harmonic peaks of the train velocity spectrum, without needing to know the applied wheel or axle load. The same principles also apply to

displacement and acceleration spectra.

## Implication for laboratory testing

The loading spectrum applied to an individual sleeper by a passing train may be represented as a complex Fourier series, with loading coefficients at multiples of the vehicle passing frequency as shown in Fig. 13.

There is a tendency for laboratory testing to be carried out at the highest obvious frequency, of consecutive axles passing. However, the analysis summarised in Fig. 13 shows that the loading component with the highest magnitude is at a lower frequency. Testing at a uniform higher frequency may lead to excessive test bed velocities or

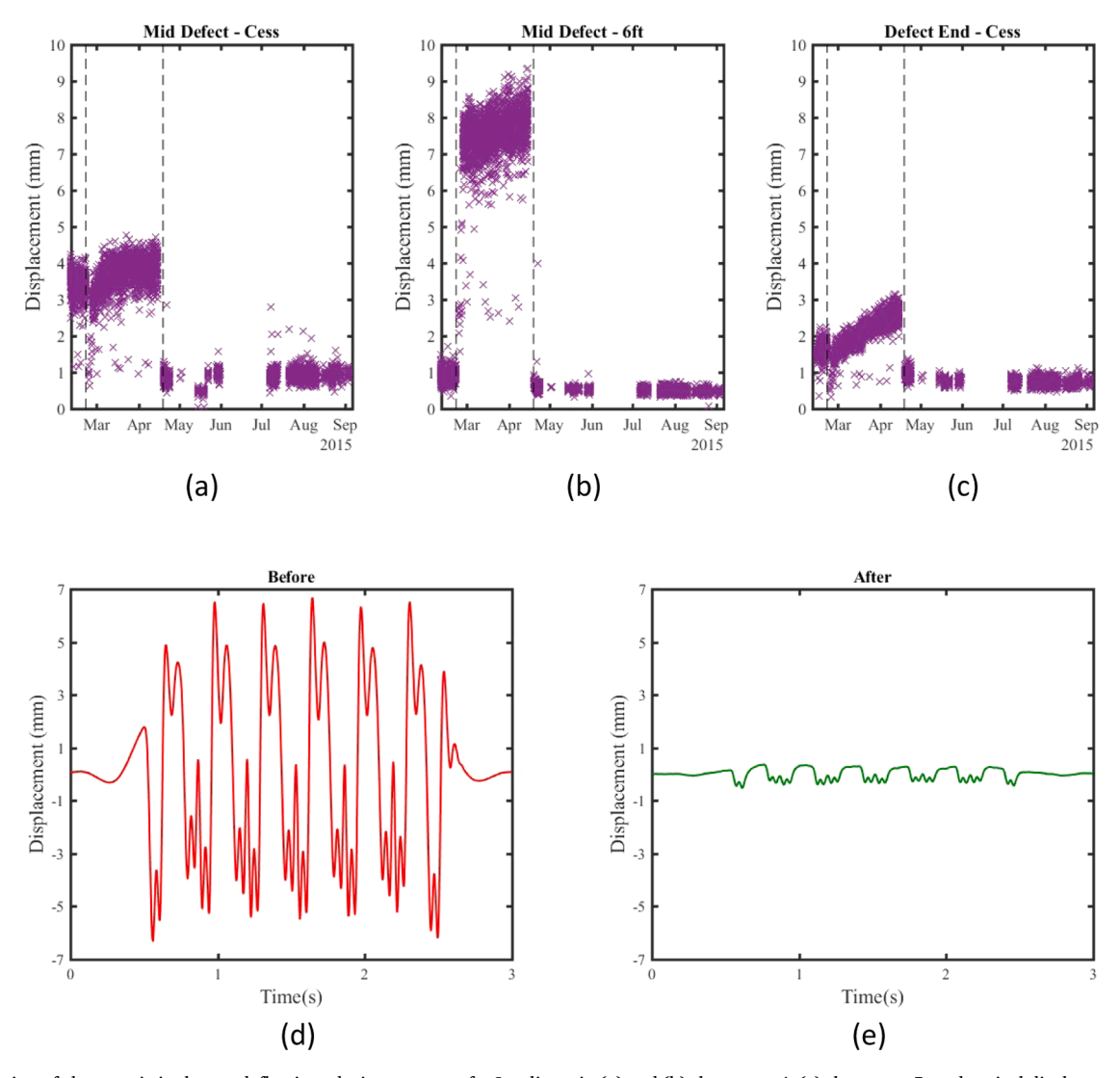


Fig. 9. Evolution of characteristic sleeper deflections during passage of a Javelin train (a) and (b) sleeper no 4, (c) sleeper no 5; and typical displacement-time traces during train passage from sleeper no.4 (d) after tamping but before the targeted repair and (e) after the targeted repair.

From Milne et al. [9].

accelerations that are not representative of service conditions. In a sophisticated testing machine, it might be possible to replicate the load spectrum, or select a cyclic test frequency that produces realistic velocities and accelerations during testing. If not, perhaps the most straightforward and controllable approach is to maintain a quasi-static test regime.

## Conclusions

- Accelerometers can be used to assess the motion and loading of railway track as trains pass. Lower frequency vibrations, typically under 40 Hz even for high-speed trains, are responsible for the most significant track movements. Some commercially-available accelerometers have become much reliable and less noisy over the past 15 years.
- 2. Signal processing and interpretation are important. Filters are required for stable integration, and artefacts from signal processing including the startup transient and shift in datum from the high pass filter need to be accounted for. Frequency content above 40 Hz is not useful for assessing displacement. Statistical and frequency domain techniques can be used to automate analysis of the datum shift

- analysis, and to assess the rail support system stiffness without knowledge of the train load.
- 3. For longer trains, dominant frequencies occur at integer multiples of the car passing frequency. This defines the loading spectrum that should be used to inform laboratory testing, although it may not always be practically feasible to apply it exactly.

## CRediT authorship contribution statement

William Powrie: Writing – review & editing, Writing – original draft, Visualization, Supervision, Resources, Project administration, Methodology, Investigation, Funding acquisition, Conceptualization. David Milne: Writing – review & editing, Supervision, Project administration, Methodology, Investigation, Formal analysis, Conceptualization. Geoff Watson: Methodology, Investigation. Ben Lee: Project administration, Investigation. Louis Le Pen: Supervision, Methodology, Investigation, Formal analysis, Data curation.

## **Declaration of competing interest**

There are no conflicts of interest.

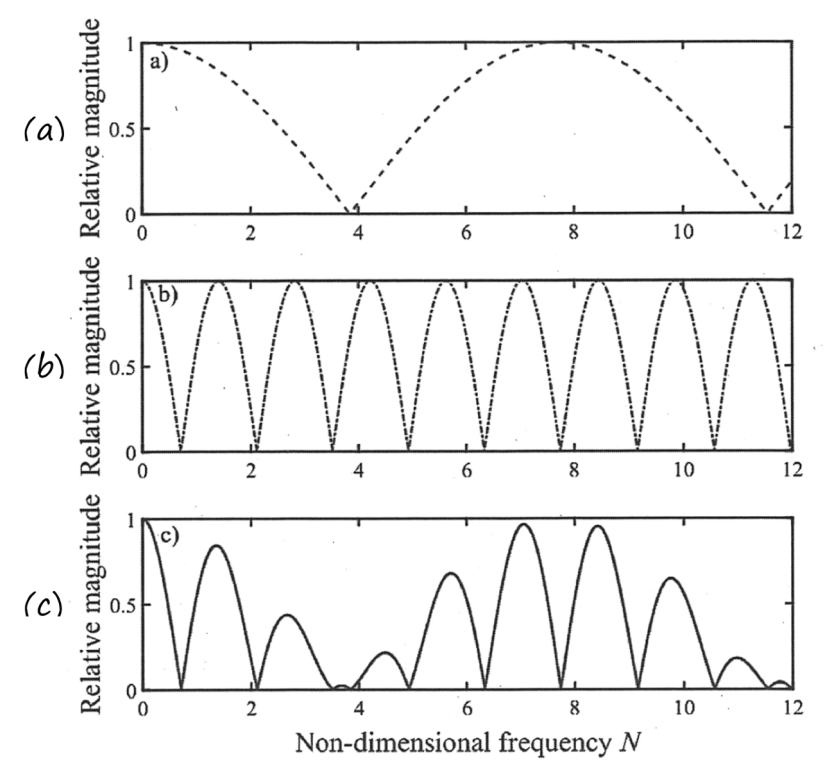


Fig. 10. Components of a single vehicle load spectrum: (a) from the axle spacing, (b) from the bogie spacing, (c) combined. From Milne et al. [7].

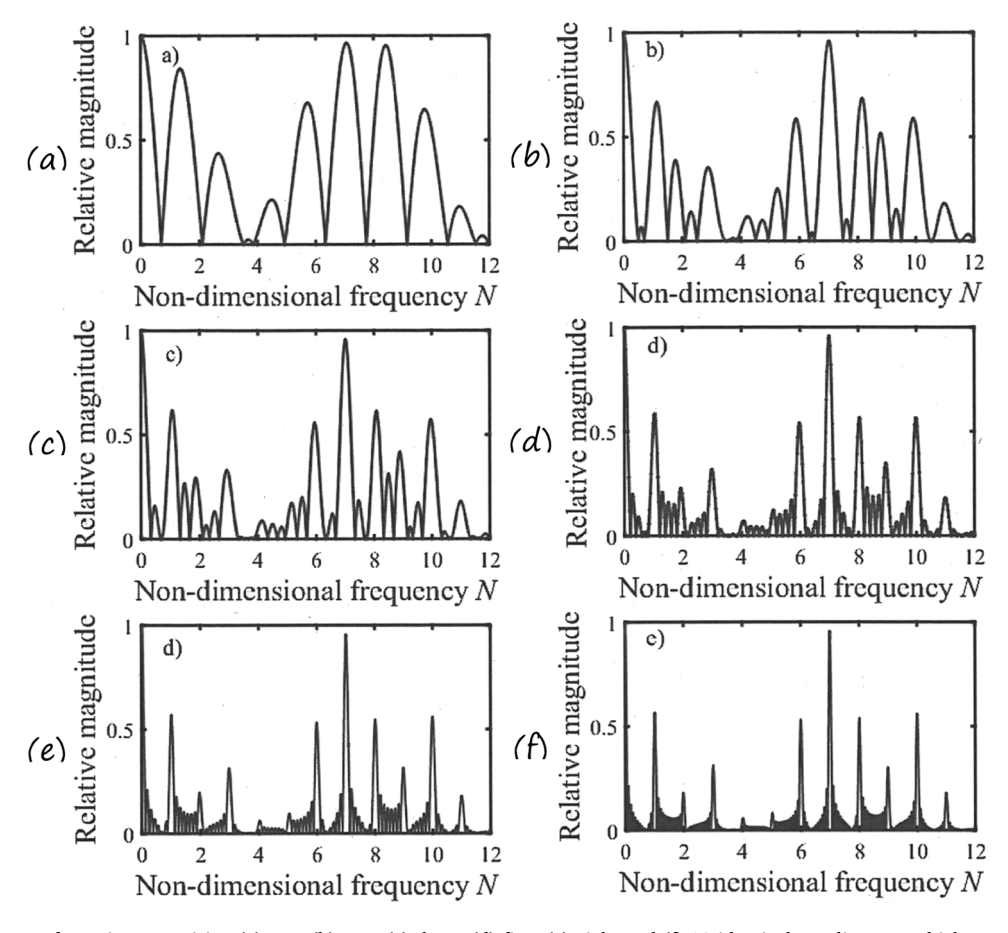


Fig. 11. Train load spectra for trains comprising (a) one, (b) two, (c) three, (d) five, (e) eight and (f) 13 identical Javelin-type vehicles. From Milne et al. [7].

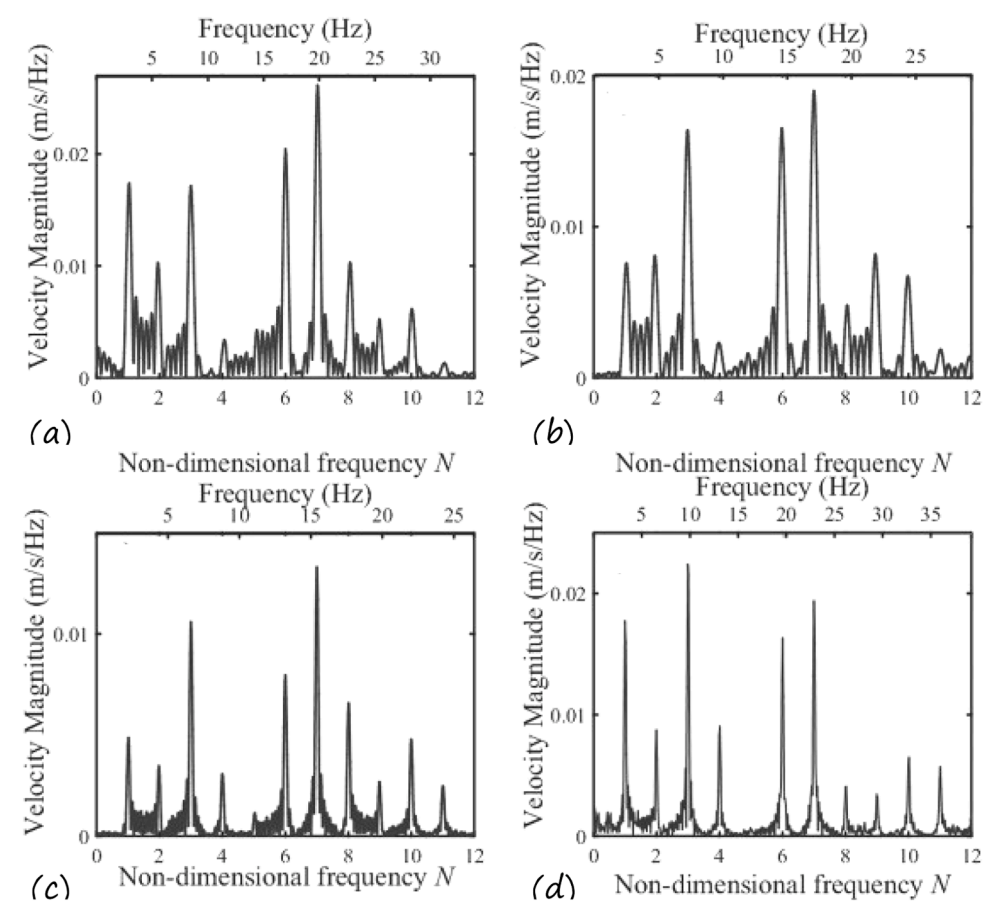
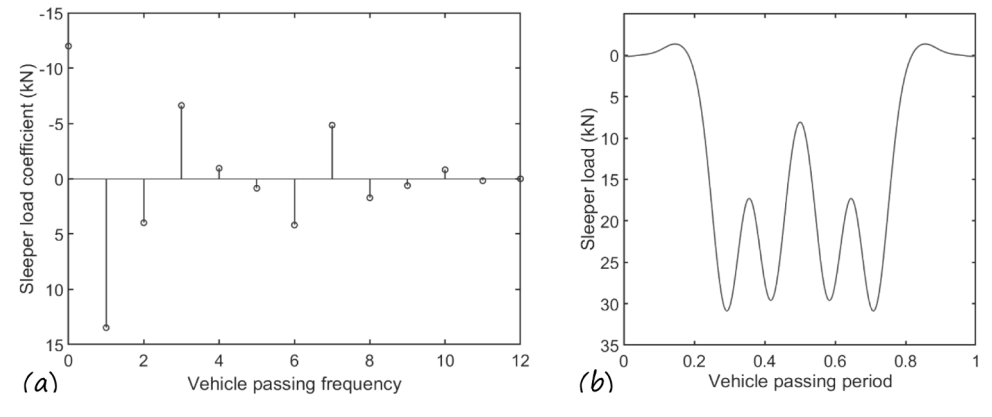


Fig. 12. Measured train load spectra for (a) a 6 car Javelin at 56.4 m/s; (b) a 5 car Voyager at 56.1 m/s; (c) an 11 car Pendolino at 54.4 m/s; and (d) a 16 car Valero at 80.8 m/s. From Milne et al. [7].



**Fig. 13.** Loading coefficients (per rail or per sleeper end) for sinusoidal loading at different multiples (harmonics) of the train vehicle passing frequency (a), making up the loading pattern experienced by each sleeper end per vehicle passage (b), for a 65 kN wheel load. From Powrie et al. [13].

## Acknowledgements

The authors acknowledge the contribution of those who have contributed to this work at the University of Southampton including David Thompson, Jeffrey Priest, Anthony Lock and the late Daren Bowness; and funders the UK Engineering and Physical Sciences Research Council, rail companies Network Rail, Network Rail Network Rail High Speed, and the European In2Rail project.

## Data availability

Data will be made available on request.

### References

- L. Auersch, The excitation of ground vibration by rail traffic: theory of vehicletrack-soil interaction and measurements on high-speed lines, J. Sound Vib. 284 (2005) 103–132, https://doi.org/10.1016/j.jsv.2004.06.017.
- [2] D. Bowness, A.C. Lock, W. Powrie, J.A. Priest, D.J. Richards, Monitoring the dynamic displacements of railway track, in: Proceedings of the Institution of

- Mechanical Engineers, Part F: Journal of Rail and Rapid Transit 221, 2007, pp. 13-22
- [3] A.C. Lamprea-Pineda, D.P. Connolly, M.F.M. Hussein, Beams on elastic foundations

   a review of railway applications and solutions, Trans. Geotechnics 33 (2022), https://doi.org/10.1016/j.trgeo.2021.100696.
- [4] L.M. Le Pen, D. Milne, D.J. Thompson, W. Powrie, Evaluating railway track support stiffness from trackside measurements in the absence of wheel of wheel load data, Can. Geotech. J. 53 (7) (2016) 1156–1166, https://doi.org/10.1139/cgj-2015-0268
- [5] L.M. Le Pen, D. Milne, G.V.R. Watson, J. Harkness, W. Powrie, A model for stochastic prediction of track support stiffness, in: Proceedings of the Institution of Mechanical Engineers Part F: Journal of Rail and Rapid Transit 234, 2019, pp. 468–481.
- [6] D. Milne, L.M. Le Pen, G.V.R. Watson, D.J. Thompson, W. Powrie, M. Hayward, S. Morley, Proving MEMS technologies for smarter railway infrastructure. Advances in transportation geotechnics 3 (ITGC 2016), Procedia Eng. 143 (2016) 1077–1084.
- [7] D. Milne, L.M. Le Pen, D.J. Thompson, W. Powrie, Properties of train load frequencies and their applications, J. Sound Vib. 397 (2017) 123–140, https://doi. org/10.1016/j.jsv.2017.03.006.
- [8] D. Milne, L.M. Le Pen, W. Powrie, D.J. Thompson, Automated processing of railway track deflection signals obtained from velocity and acceleration measurements,

- Proc. Inst. Mech. Eng. Part F J. Rail Rapid Transit 232 (8) (2018) 2097–2110, https://doi.org/10.1177/0954409718762172.
- [9] D. Milne, L.M. Le Pen, G.V.R. Watson, D.J. Thompson, W. Powrie, M. Hayward, S. Morley, Monitoring and repair of isolated trackbed defects on a ballasted railway, Trans. Geotechnics 17 (A) (2018) 61–68, https://doi.org/10.1016/j. trgeo.2018.09.002.
- [10] D. Milne, J. Harkness, L. Le Pen, W. Powrie, The influence of variation in track level and support system stiffness over longer lengths of track on track performance and vehicle track interaction, Veh. Syst. Dyn. 59 (2) (2019) 245–268.
- [11] J.A. Priest, W. Powrie, Determination of dynamic track modulus from measurement of track velocity during train passage, J. Geotech. Geoenviron. Eng. 135 (11) (2009) 1732–1740, https://doi.org/10.1061/(ASCE)GT.1943-5606.0000130.
- [12] S. Timoshenko, B.F. Langer, Stresses in railroad track, ASME. Trans. ASME 54 (2) (1932) 277–293, https://doi.org/10.1115/1.4021826.
- [13] W W. Powrie, L.M. Le Pen, D. Milne, D.J. Thompson, Train loading effects in railway geotechnical engineering: ground response, analysis, measurement and interpretation, Trans. Geotechnics 21 (2019) 100261, https://doi.org/10.1016/j. trgeo.2019.100261.
- [14] Y. Tang, Q. Yang, X. Ren, S. Xiao, Dynamic response of soft soils in high-speed rail foundation, Can. Geotech. J. 56 (2019) 1832–1848, 2019.